Sidewall alkylcarboxylation of carbon nanotubes through reactions of fluoronanotubes with functional free radicals*

*O. V. Kuznetsov,[a] A. Cole,[b] M. Pulikkathara,[b] and V. N. Khabashesku[c]**

[a]*Department of Physics and Astronomy,*
[b]*Department of Chemistry,*
[a,b]*Rice University, 6100 Main Street, Houston, Texas 77005, USA*
[c]*Department of Chemical and Biomolecular Engineering,*
University of Houston, 4800 Calhoun blvd., Houston, Texas 77204, USA.
Fax: (713) 743 4323. E-mail: valery@uh.edu

Addition of carboxyalkyl radicals to carbon nanotube (CNT) graphene surface is a non-destructive to nanotube framework method of sidewall functionalization of CNTs with the carboxylic group terminated moieties. Fluorination activates the CNT surface towards addition reactions due to transformation of the graphene aromatic structure to a more chemically reactive polyene π-system structure of fluoronanotubes. As a result, the sidewall addition reactions to fluoronanotubes are completed in a much shorter time spans than in the case of pristine CNTs. Carboxyalkyl CNT derivatives prepared by this method form stable suspensions in water and polar organic solvents. This enables their applications in biomedical research; for the preparation of water-based paints, inks, and coatings; and for processing and fabrication of nanocomposites.

Key words: carbon nanotubes, free radicals, sidewall functionalization, solubilization.

Carbon nanotubes (CNTs) possess unique mechanical, electrical, optical, and thermal properties which offer a wide range of opportunities for their application.[1—7] However, many promising engineering and biomedical applications of CNTs can be realized only when the tendency of CNTs to form tight bundles and ropes is overcome by functionalization. Along with the separation of individual nanotubes from their bundles, the functionalization would also improve the dispersion and solubilization of the CNTs in common organic solvents and water needed for their processing and manipulation. To solve this problem, the approaches based on non-covalent[8—14] and covalent[15—20] functionalization of nanotubes are being pursued. The non-covalent functionalization is generally used when CNT electrical and optical properties need to be maintained. The covalent functionalization leads to attachment of various functional groups to the ends or side walls of the nanotubes through covalent bonds. Functionalization of the nanotube ends brings only a highly localized transformation of the nanotube electronic structure and does not change the bulk properties of these materials. The oxidation reactions forming shortened nanotubes with carboxylic acid groups at the ends have been the most extensively used for this type of functionalization.[21—24] On the contrary, functionalization of the nanotube side walls naturally results in a significant modification of the intrinsic properties of the nanotubes.

The challenges faced in the sidewall chemical functionalization are related to a very low reactivity of the nanotubes due to a much lower curvature of nanotube graphene walls than in the fullerenes and to the necessity of preserving the tubular structure when attaching the functional groups. The carbon nanotube graphene structure built from carbon atoms in their sp^2-bonding states facilitates the predominant occurrence of additional reactions. For this type of reactions, gaseous fluorine serves as a reagent of choice, since it easily generates highly reactive F atoms under mild conditions (the F—F bond dissociation energy is only 158 kJ mol^{-1}) and, therefore, controlled fluorination became the most powerful tool for surface modification of CNTs at large scales.[16,19,20] Other addition reactions of CNTs involve reactive molecules and transient species such as azomethine ylides,[25] aryl-substituted carbenes and nitrenes,[25] and organic free radicals generated from either diazonium salts,[15] or acyl peroxides.[26—29] The importance of this group of functionalization methods is that they are non-destructive to the CNT side walls as compared to widely used oxidative treatments which cause the sidewall etching and degradation of mechanical strength of the nanotube. In this regard, the addition of free radicals generated from acyl peroxides to

* Dedicated to Academician of the Russian Academy of Sciences O. M. Nefedov on the occasion of his 80th birthday.

Published in Russian in *Izvestiya Akademii Nauk. Seriya Khimicheskaya,* No. 11, pp. 2170—2179, November, 2011.
1066-5285/11/6011-2212

pristine single-walled carbon nanotubes (SWCNTs) is particularly important, since they provide a simple one-step functionalization route using a commercially available low-cost reagents. This approach has successfully been demonstrated through additive reactions of phenyl and undecyl radicals, generated[26] from benzoyl and lauroyl peroxides, respectively, and functional radicals, such as carboxyethyl (**1**$^{\bullet}$) and carboxypropyl (**2**$^{\bullet}$), produced from succinic (**3**) and glutaric acid peroxides (**4**) with SWCNTs.[27] Making use of radicals **1**$^{\bullet}$ and **2**$^{\bullet}$ in these reactions is especially valuable since they lead to the CNTs sidewall functionalized with the alkyl moieties terminated with the carboxylic acid groups, which in their turn can further be modified for specific applications.[27,30] However, the large-scale utility of this functionalization method is held back by a low reaction rate of the addition of carboxyethyl (**1**$^{\bullet}$) and carboxypropyl (**2**$^{\bullet}$) radicals to the side walls of the nanotubes. For example, a mixture of SWCNTs with peroxides **3** or **4** needs to be heated at 80—90 °C for 5—10 days while adding every day a tenfold excess of acyl peroxide. Therefore, finding the way of accelerating this process is necessary in order to increase its commercial importance.[27,31]

The DFT calculations suggested[32] that the fluorinated CNTs (fluoronanotubes, F-CNTs) are better electron acceptors than the bare carbon nanotubes and, therefore, they should more strongly interact with the electron-rich molecules and transient species, including free radicals. In our previous study[26] we have shown that the sidewall C—C bonding reactions of undecyl ($C_{11}H_{23}$) and phenyl radicals proceeded more efficiently in the case of F-SWCNTs than pristine SWCNTs, as indicated by a much lower reaction time (3 h instead of 5 days). This is explained by the fact that fluorination causes transformation of the graphene aromatic structure of pristine CNTs to a more chemically reactive polyene π-system structure in the fluoronanotubes and, as a result, activates the CNT surface towards additional reactions. Being encouraged by these preliminary results, in the present work we have studied the fluorinated CNTs, both single- and multi-walled, as "activated" precursors for the addition of functional **1**$^{\bullet}$ and 1-cyano-1-methyl-3-carboxypropyl (**5**$^{\bullet}$) radicals thermally generated from peroxide **3** and 4,4-azobis-(4-cyanovaleric acid) (**6**), respectively.

Experimental

Materials. Fluorinated SWCNTs (F-SWCNTs, batch F-0219-1) and pristine carbon nanotubes (batch no. XD3365A) were purchased from Carbon Nanotechnologies, Inc (at present Unidym). These nanotubes were synthesized from CO under a high pressure through the HipCO process originally invented at Rice University and then commercialized by this company.[10a] The X-ray photoelectron spectroscopy (XPS) analysis of the F-SWCNTs done on at least five spots of the sample yielded an average C_2F stoichiometry for this fluorocarbon. Electron probe microanalysis of the solid residue of the F-SWCNT subjected to TGA revealed ~0.2 at.% Fe. Atomic force microscopy (AFM) analysis has shown that more than 90% of these F-SWCNTs are relatively short, with the length distribution in the range of 200—700 nm and an average diameter of about 1.3 nm.

Approximately two thirds of the XD class carbon nanotube material (XD-CNT) are made of single-walled and one third is composed of double- and multi-walled carbon nanotubes and the material also contained about 4 wt.% of the iron catalyst. The lengths of XD-CNTs were within 1—3 μm and diameters were in the range from 1 to 4 nm. Multi-walled carbon nanotubes (MWCNTs) with outside diameters of 20—40 (sample A) and 60—100 nm (samples B) were purchased from Nanostructured and Amorphous Materials, Inc. All CNTs were used without any further purification. Fluorine—helium mixtures were purchased from Spectra Gases. Succinic acid anhydride and 4,4-azobis-(4-cyanovaleric acid) (**6**) were acquired from ACROS Organics.

Methods. The nanocarbon materials XD-CNTs and MWCNTs were fluorinated in a custom-built fluorination apparatus described elsewhere.[16,20] The XD-CNTs were fluorinated at 150 °C by using an F_2/He (1 : 10) mixture to an approximately C_5F stoichiometry estimated from weight gain. The fluorination of MWCNTs was carried out by 20% F_2—80% He mixture at 150 and 250 °C for 2 h followed by annealing in a helium flow for 6 h. After fluorination of MWCNTs the measured weight gains due to fluorine addition at different temperatures were the following: 17% (150°C) and 27% (250 °C) for sample A, 11% (150 °C) and 10% (250 °C) for sample B.

Succinic acid peroxide (**3**) was prepared through the treatment of succinic acid anhydride with 8% hydrogen peroxide according to a previously described procedure.[27]

Ethylcarboxylation of fluorinated carbon nanotubes (general procedure). Fluorinated nanotubes (F-SWCNTs, F-XD-CNTs, or F-MWCNTs (A or B)) (100 mg) were dispersed in *o*-dichlorobenzene (100 mL), peroxide **3** (1 g) was added, and the mixture was stirred for 12—16 h at 90 °C. After cooling the reaction mixture to room temperature, THF (50 mL) was added, and the mixture was sonicated for 1 h followed by filtration through Teflon membrane (diameter 0.22 μm). The precipitate remained on the membrane was washed with ethanol, and the product was dried in a vacuum oven for 12 h.

Cyanopropylcarboxylation of nanotubes F-SWCNTs and F-XD-CNTs. A sample weight (50 mg) was dispersed in *o*-dichlorobenzene, compound **6** (0.5 g) was added, and the mixture was stirred for 24 h at 80 °C followed by a similar work-up procedure as that for compound **3**.

Characterization. Fluorinated and alkylcarboxylated CNT materials were characterized by FTIR, Raman, TGA, XPS, and scanning electron microscopy (SEM) methods. The FTIR spectral measurements were performed using a Thermo Nicolet Nexus 670 FTIR spectrometer. The spectra were collected either in a transmission mode from samples pressed into KBr pellets or in a reflective mode from neat powders placed on the surface of diamond crystals in the Golden Gate ATR accessory. The Raman spectra were collected with a Renishaw 1000 Microraman system operating with a 780-nm laser source. Thermogravimetric analysis was carried out with a TA-SDT-2960 analyzer by heating samples in platinum pans from 20 to 800 °C in argon atmosphere. The XPS data were collected with a PHI Quantera X-ray

photoelectron spectrometer using a monochromatic AlKα radiation source with a power of 95.4 W and an analyzer with a pass energy of 26 eV. To examine surface morphology, scanning electron microscopy was used at 30 kV beam energy in a high-vacuum mode using a FEI Quanta 400 ESEM FEG instrument.

Solubility determination. The quantitative estimation of solubility was done by dispersing 25 mg of each alkylcarboxylated CNT sample in 50 mL of de-ionized water followed by standing for one week. Then the top 40 mL of each solution were decanted, and the solid precipitate was separated from the rest of the solutions by filtration through the membrane, dried *in vacuo* for 12 h, and then weighed.

Results and Discussion

Reactions of fluoronanotubes with functional free radicals. These reactions proceed by addition of organic free radicals to polyene π-bonds in the fluoronanotubes followed by elimination of fluorine atoms which can form HF or alkyl fluorides as final products. Carboxyalkyl radicals **1**$^{\bullet}$ and **5**$^{\bullet}$ generated from acyl peroxides **3** and **6** (Scheme 1), respectively, were anticipated to show lower reactivity than undecyl ($C_{11}H_{23}$) or phenyl radicals studied earlier in the reactions with fluoronanotubes.[26] This is most likely related to the presence of electron-withdrawing carboxyl and cyano groups in their structures. Since radical **5**$^{\bullet}$ contains both groups, it was expected that this radical will also be somewhat less reactive than radical **1**$^{\bullet}$. The experimental data obtained in the present work are in line with these estimations.

Indeed, it was found that carboxyethyl radicals generated from compound **3** reacted with fluorinated single- and multi-walled carbon nanotubes within 12—16 h, while in the case of undecyl ($C_{11}H_{23}^{\bullet}$) and phenyl radicals only 3 h were sufficient for the similar reactions to complete.[26] Nevertheless, these reaction times are already much shorter than needed for completion of the reactions of radicals **1**$^{\bullet}$ with pristine carbon nanotubes (at least 120 h).[27] At the same time, radicals **5**$^{\bullet}$ produced from compound **6** did not form adducts with pristine carbon nanotubes studied. However, radicals **5**$^{\bullet}$ were found to readily react with fluorinated carbon nanotubes, although during a longer time (24 h) than radicals **1**$^{\bullet}$ react and produce the addition products F-SWCNT·**5**$^{\bullet}$ and F-XD-CNT·**5**$^{\bullet}$. These conclusions on the relative reactivity of carboxyalkyl radicals studied in the present work have been supported by the characterization data obtained using spectroscopy, thermal gravimetric analysis, and electron microscopy of final addition products.

Raman spectroscopy. Useful information on the degree of modification of the CNT sidewall in relation to the type and size of the CNTs studied and a chemical modification agent used can be obtained with the help of Raman spectroscopy. In the Raman spectra of CNTs the D band near ~1300 cm^{-1} is attributed to disordered graphite structures or sp^3-hybridized carbon atoms of the nanotubes, whereas the G band at ~1600 cm^{-1} corresponds to a splitting of the E_{2g} stretching mode of graphite, which reflects the structural intensity of the sp^2-hybridized carbon atoms. The increase in the band intensity ratio (I_D/I_G) for the functionalized carbon nanotubes reflects the relative degree of covalent functionalization or defects in the nanotubes.[33] For instance, comparison of the Raman spectra (Figs 1 and 2) of the F-SWCNTs and F-XD-CNTs fluorinated to a different bulk stoichiometries (C_2F and C_5F, respectively) clearly shows a much higher degree of surface functionalization of the F-SWCNTs. This is demon-

Scheme 1

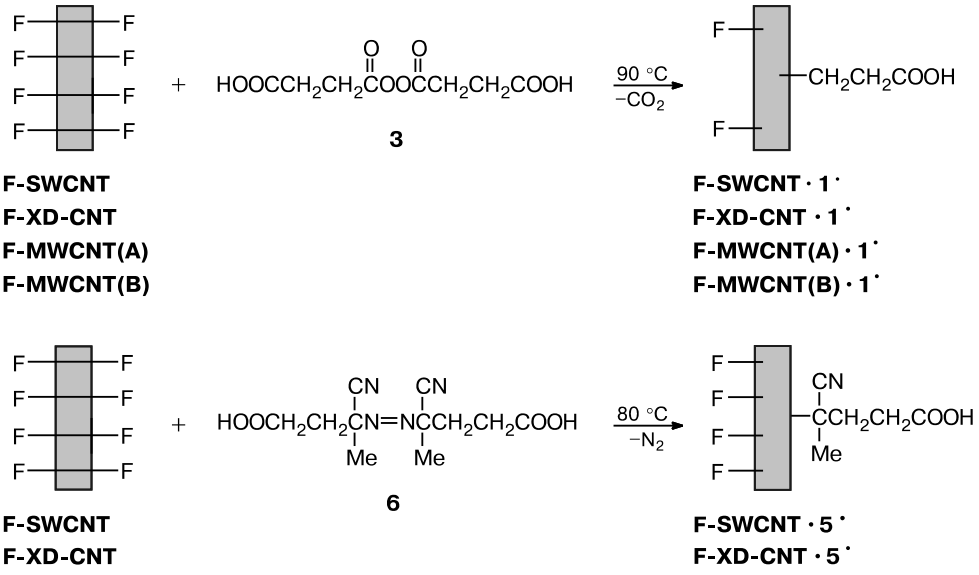

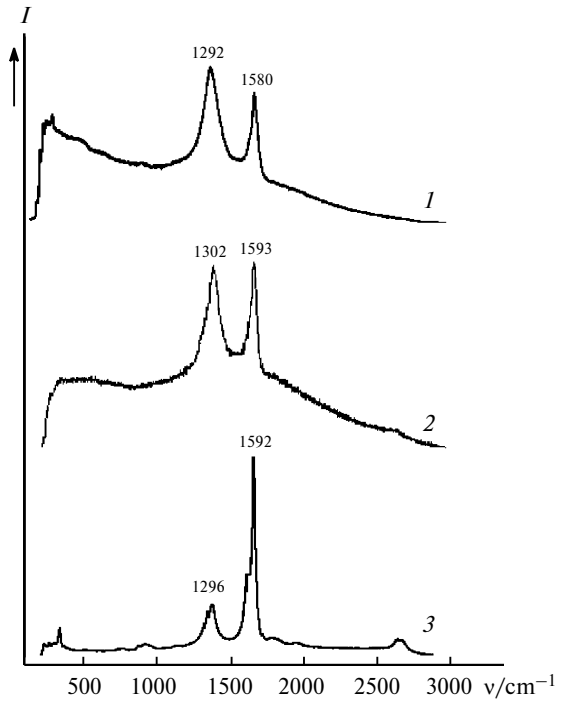

Fig. 1. Raman spectra (λ = 780 nm) of functionalized CNTs: F-SWCNT (*1*), F-SWCNT·**1**˙ (*2*), and F-SWCNT·**5**˙ (*3*).

strated by a much higher intensity of the D-mode peak near ~1300 cm^{-1} in the spectrum of F-SWCNT (see Fig. 1, curve *1*), as compared to the corresponding peak in the spectrum of F-XD-CNT (see Fig. 2, curve *1*).

The Raman spectra of alkylcarboxylated CNTs, F-SWCNT·**1**˙ (Fig. 1, curve *2*), and F-SWCNT·**5**˙ (see Fig. 1, curve *3*) show the upshifts of the D peak by 10 and 4 cm^{-1}, respectively, and the G peak (by 12—13 cm^{-1}) relatively to fluoronanotubes, which indicate that another groups have been attached to the SWCNT side walls. These spectra also show a decrease in the D peak intensity, which is related to an overall reduction of the number of sp^3 C—C bonding sites due to partial defluorination, accompanied by the recovery of the sp^2 C=C aromatic bonds between the sites of C—C bonding of carboxyalkyl groups to the nanotube side walls.

In comparison with F-SWCNTs, the D-mode band in the Raman spectrum of F-XD-CNTs (see Fig. 2, curve *1*) appears at a higher frequency, which is most likely due to the presence of a large fraction of fluorinated double-walled nanotubes (DWCNTs) and F-MWCNTs in the sample. This is reasonable assumption since in the Raman spectra of F-MWCNT(A) (Fig. 3, *a*, curve *1*) and F-MWCNT(B) (Fig. 3, *b*, curve *1*) the band of D mode appears at positions 17—20 cm^{-1} higher than those in F-SWCNTs, which can be explained by a reduced surface curvature in MWCNTs. The decrease in the intensity of the D-mode peak with respect to the G-mode peak observed in the Raman spectra of adducts F-XD-CNT·**1**˙ (see Fig. 3,

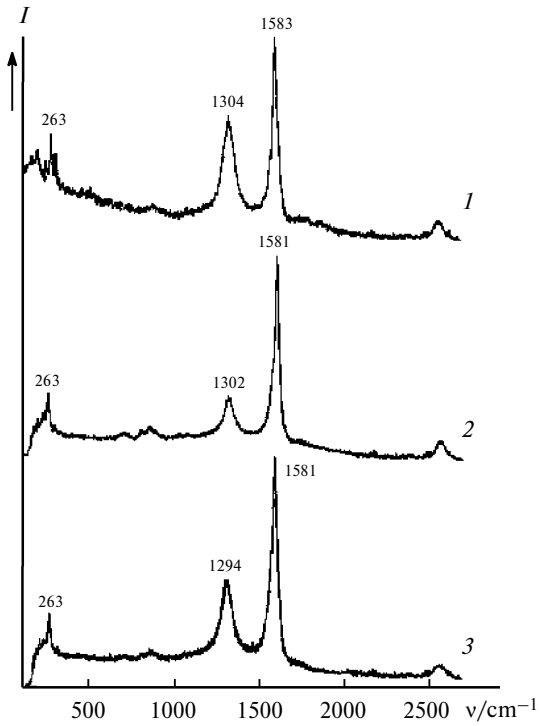

Fig. 2. Raman spectra (λ = 780 nm) of functionalized XD-CNTs: F-XD-CNT (*1*), F-XD-CNT·**1**˙ (*2*), and F-XD-CNT·**5**˙ (*3*).

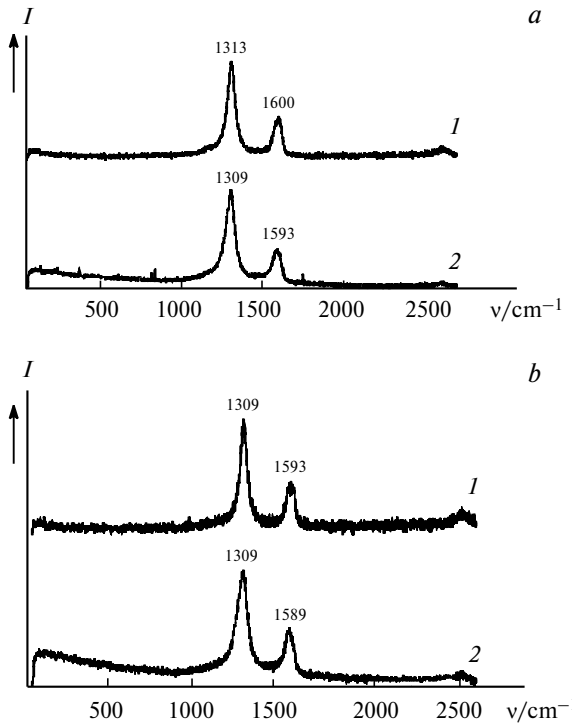

Fig. 3. Raman spectra (λ = 780 nm) of functionalized MWCNTs: (*a*) F-MWCNT(A) (*1*) and F-MWCNT(A)·**1**˙ (*2*); (*b*) F-MWCNT(B) (*1*) and F-MWCNT(B)·**1**˙ (*2*).

curve *2*) and F-XD-CNT•**5**˙ (see Fig. 3, curve *3*) can be attributed to partial removal and substitution of F groups by moieties **1**˙ and **5**˙ in F-XD-CNTs occurring by analogy to F-SWCNTs.

It was noted[34] that, in contrast to SWCNTs, the separated bands in the Raman spectra of MWCNTs are more difficult to identify, because the difference of band positions decreases with an increase in the tube diameter and the presence of multiple concentric tubes. Also, the presence of high density of sidewall defects in neat MWCNTs and in F-MWCNT(A) and F-MWCNT(B), as demonstrated by their SEM images (Fig. 4), further complicates the identification of surface chemical modification of MWCNTs. The Raman spectra of the fluorinated MWCNTs (see Fig. 3, *a*, *b*, curves *1*) look quite similar to the spectra of respective ethylcarboxylated derivatives F-MWCNT(A)•**1**˙ (see Fig. 3, *a*, curve *2*) and F-MWCNT(B)•**1**˙ (see Fig. 3, *b*, curve *2*) in band intensity ratio (I_D/I_G). They, however, differ in observed downshifts of the D-mode and G-mode peak positions in the spectra of F-MWCNT(A) by 4 and 7 cm^{-1}, respectively, (see Fig. 3, *a*, curve *2*), and G-mode peak in F-MWCNT(B)•**1**˙ by 4 cm^{-1} with respect to F-MWCNTs (Fig. 3). This provides an indication of a change in the chemical bonding environment around sp^3-carbon atoms on the outer surface of functionalized MWCNTs.

FTIR spectroscopy. Structural information on the functional groups bonded to the surface of carbon nanotubes before and after the alkylcarboxylation reaction was obtained from the FTIR spectra. In the ATR-FTIR spectrum of the F-SWCNT sample (Fig. 5, curve *1*), the absorption band of the C—F stretch was observed at 1147 cm^{-1}, while the band of activated sidewall C=C stretches appears near 1559 cm^{-1} in agreement with the IR characterization data on fluorinated HipCO SWCNTs.[16,20]

In the ATR-mode spectrum of F-SWCNT•**1**˙ (see Fig. 5, curve *2*) the band of O—H stretch of carboxyl groups was not clearly seen, although a notable peak of the C=O stretch was observed at 1720 cm^{-1}. A group of peaks in the 2800—3000 cm^{-1} interval are due to the C—H stretches of the carboxyethyl functional groups. Peaks observed at 1571 cm^{-1} and in the 1300—1460 cm^{-1} region are related to sidewall C=C stretching and carboxyethyl C—H bending motions, respectively, while a broad high intensity band peaking at 1165 cm^{-1} is most likely due to C—C stretches of the carboxyethyl groups.[27] In contrast, a broad peak due to O—H stretch was observed in the 3000—3400 cm^{-1} region of the ATR-FTIR spectrum (see Fig. 5, curve *3*) of

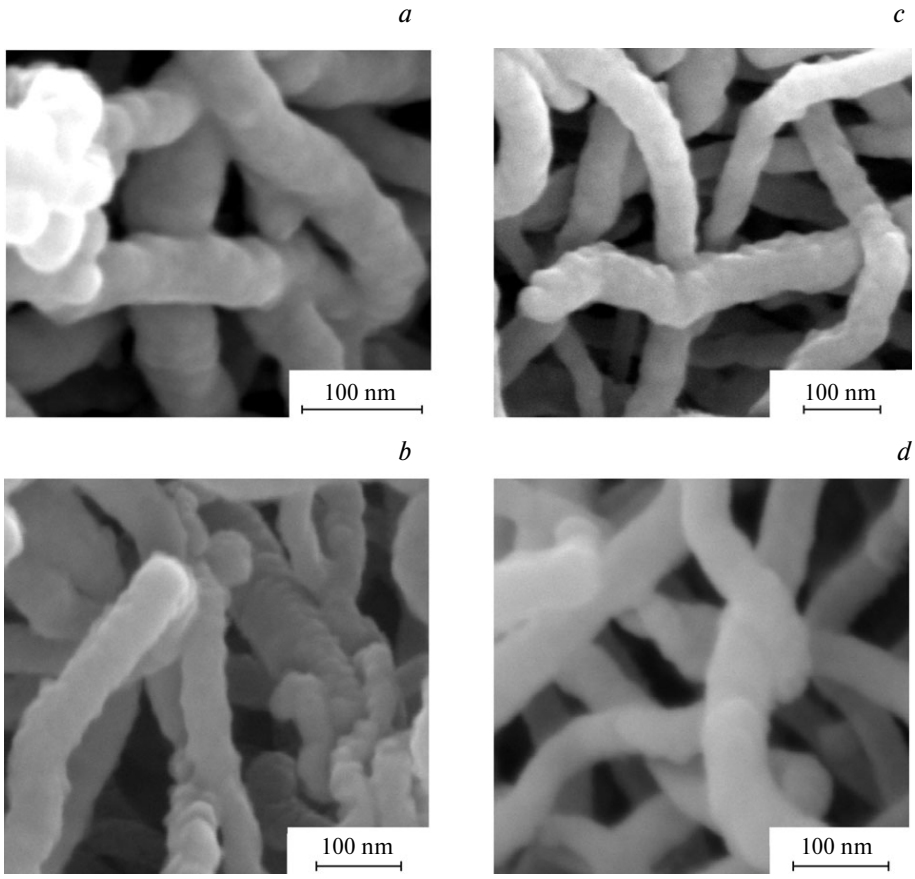

Fig. 4. SEM images of CNTs: MWCNT(A) (*a*), F-MWCNT(A) (*b*), MWCNT(B) (*c*), and F-MWCNT(B) (*d*).

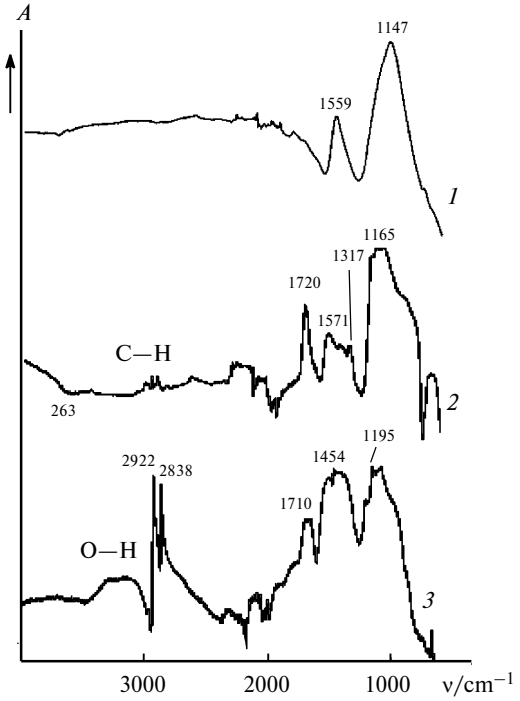

Fig. 5. ATP-FTIR spectra of functionalized SWCNTs: F-SWCNT (*1*), F-SWCNT·**1**˙ (*2*), and F-SWCNT·**5**˙ (*3*).

F-SWCNT-**5**˙ derivative. This spectrum has also exhibited the other signatures of groups **5**˙: C—H stretches, appearing as a pair of high-intensity peaks at 2838 and 2922 cm^{-1}, the C=O stretch at 1710 cm^{-1} as a mid-intensity band, C—H bending mode at 1454 cm^{-1}, and C—C stretch at 1195 cm^{-1}.

The FTIR spectra of XD-CNTs (Fig. 6) and MWCNTs (Fig. 7) derivatives were collected from samples mixed with KBr and pressed into pellets. This resulted in observation of better resolved bands in the spectra of F-XD-CNT·**1**˙ and F-XD-CNT·**5**˙ (Fig. 6) due to reduced interaction between functionalized nanotubes dispersed in KBr matrix as compared to neat samples studied in the ATR mode.

The O—H stretches of carboxyalkyl groups have been observed as strong bands at 3462 and 3437 cm^{-1} and C=O stretches as medium-intensity bands at 1726 and 1720 cm^{-1} in the KBr FTIR spectra of F-XD-CNT·**1**˙ (see Fig. 6, curve *2*) and F-XD-CNT·**5**˙ (Fig. 6, curve *3*), respectively. Weak but clearly seen bands of the C—H stretches were noted in the 2800—3000 cm^{-1} regions of these spectra. Bands due to sidewall C=C stretches in each derivative were located at 1559 cm^{-1} (see Fig. 6, curve *1*), 1577, and 1549 cm^{-1}. Broad prominent peaks at 1147, 1167, and 1154 cm^{-1} were attributed to C—F stretches of functional groups in F-XD-CNTs and C—C stretches of functional groups in F-XD-CNT·**1**˙ and F-XD-CNT·**5**˙, respectively. Very weak absorption at 2093 cm^{-1} in the spectrum of derivative **5**˙ is likely due to

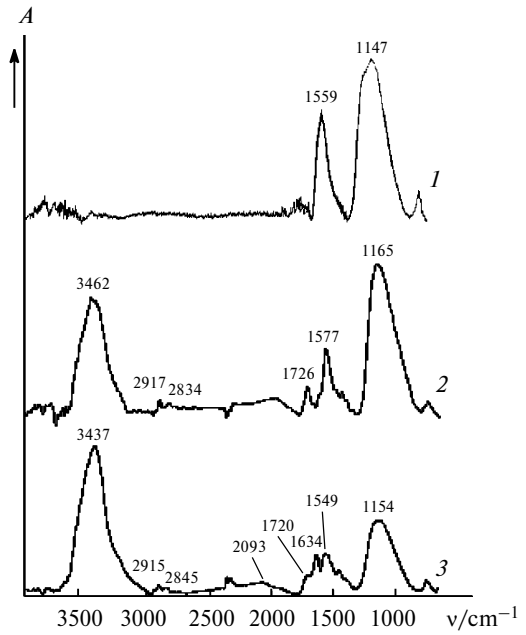

Fig. 6. FTIR spectra of functionalized CNTs: F-XD-CNT (*1*), F-XD-CNT·**1**˙ (*2*), and F-XD-CNT·**5**˙ (*3*).

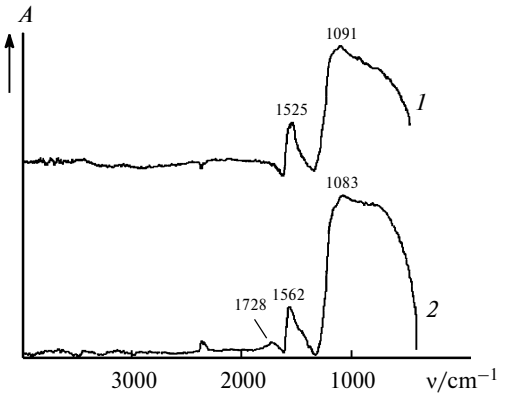

Fig. 7. FTIR spectra (in KBr) of functionalized MWCNTs: F-MWCNT($A_{250\,°C}$) (*1*) and F-MWCNT($A_{250\,°C}$)·**1**˙ (*2*).

C≡N stretch mode significantly downshifted from its typical position near 2250 cm^{-1} because of possible strong interaction of the C≡N groups with the CNT sidewall surface, while band at 1634 cm^{-1} can be related to adsorbed moisture.

As compared to SWCNTs, clear absorptions of surface bonded groups in the FTIR spectra of all functionalized MWCNTs were observed only in the regions below 2000 cm^{-1} as demonstrated by selected spectra of MWCNTs fluorinated at 250 °C (see Fig. 7, curve *1*) and then ethylcarboxylated (see Fig. 6, curve *2*). In the former spectrum, the band at 1525 cm^{-1} belongs to the sidewall C=C stretch, while the broad band at 1091 cm^{-1} belongs to the C—F stretch. In the latter spectrum, weak absorption at 1728 cm^{-1} can be attributed to the C=O stretch of

the carboxyethyl groups and bands at 1562 and 1083 cm^{-1} belong to the sidewall C=C stretch and C—C stretch of the carboxyethyl groups, respectively.

XPS analysis. This method is known to provide information on surface elemental composition and atomic bonding environment in the materials by sampling at only a few nanometers depth from the solid surface. The elemental analysis data obtained by XPS are summarized in Table 1. These data confirm fluorine removal from F-SWCNTs and F-MWCNTs after treatment with free radical precursors **3** and **6**. This detachment can occur both through displacement by radicals **1**$^{\bullet}$ and **5**$^{\bullet}$, respectively, and defluorination reactions by showing a reduced fluorine content in all alkylcarboxylated CNTs. The largest decrease in the fluorine content (from 35.7 to 8.9%) among the materials analyzed by XPS was found for F-CNT$\cdot$**5**$^{\bullet}$. At the same time, oxygen and nitrogen contents due to surface bonded functional groups **5**$^{\bullet}$ were found to be as low as 5.7 and 0.9%, respectively. This clearly indicates a considerable contribution of defluorination to the reaction of cyanopropylcarboxylation of F-SWCNTs, since if this reaction would result only in substitution of fluorine for radical **5**$^{\bullet}$, then the fluorine content should have been reduced by no more than 3 at.% after the reaction. Based on XPS elemental analysis data, the degree of surface functionalization in F-CNT$\cdot$**5**$^{\bullet}$ derivative was calculated as one group **5**$^{\bullet}$ in 70 carbon atoms.

Among ethylcarboxylated MWCNTs, the most notable (7.1 and 6.2 at.%) loss in fluorine content was observed for F-MWCNT($A_{150\,°C}$)$\cdot$**1**$^{\bullet}$ and F-MWCNT($B_{150\,°C}$)$\cdot$**1**$^{\bullet}$ derivatives, respectively. Oxygen content in these materials, mostly due to carboxyethyl surface groups **1**$^{\bullet}$ was found to be 6.1 and 4.4 at.%, respectively. These XPS data show that loss in fluorine content due to defluorination is much less evident in the case of MWCNT derivatives than in similarly functionalized SWCNTs. At the same time, fluorine substitution is more or less equally pronounced, resulting in degrees of surface functionalization (R/C) by groups **1**$^{\bullet}$ of 1 : 19 for F-MWCN($A_{150\,°C}$)$\cdot$**1**$^{\bullet}$ and 1 : 28 for F-MWCNT($B_{150\,°C}$)$\cdot$**1**$^{\bullet}$. These slight differences in R/C values are in line with the expected lower reactivity of large diameter (60—100 nm) F-MWCNT($B_{150\,°C}$), having lower surface curvature than smaller diameter (20—40 nm) F-MWCNT($A_{150\,°C}$).

Table 1. XPS elemental analysis data on fluorinated and alkylcarboxylated CNTs (at.%)

Sample	C1s	F1s	O1s	N1s
F-SWCNT	64.3	35.7	—	—
F-SWCNT$\cdot$**5**$^{\bullet}$	84.5	8.9	5.7	0.9
F-MWCNT($A_{150\,°C}$)	73.2	26.8	—	—
F-MWCNT($A_{150\,°C}$)$\cdot$**1**$^{\bullet}$	74.2	19.7	6.1	—
F-MWCNT($A_{250\,°C}$)	69.6	29.4	—	—
F-MWCNT($A_{250\,°C}$)$\cdot$**1**$^{\bullet}$	72.7	24.8	2.6	—
F-MWCNT($B_{150\,°C}$)	73.0	27.0	—	—
F-MWCNT($B_{150\,°C}$)$\cdot$**1**$^{\bullet}$	74.7	20.8	4.4	—
F-MWCNT($B_{250\,°C}$)	65.5	34.6	—	—
F-MWCNT($B_{250\,°C}$)$\cdot$**1**$^{\bullet}$	65.4	31.2	3.4	—

Figure 8 shows, as a selected example, the high-resolution XPS C1s, O1s, and F1s spectra for F-MWCNT-($A_{150\,°C}$)$\cdot$**1**$^{\bullet}$ derivative prepared from MWCNT(A) material fluorinated at 150 °C.

Curve-fitting analysis of the peaks helped to evaluate the bonding environment of atoms composing the surface structure of this functionalized MWCNT. In the C1s spectrum (see Fig. 8, *a*) the most intense peak at 283.9 eV has been attributed to the C—H bonded carbon atoms of functional groups **1**$^{\bullet}$, while peaks at 284.3 and 285.8 eV were assigned to carbons forming the sidewall C=C and C—O bonds in moieties **1**$^{\bullet}$, respectively. Carbon atoms bonded to fluorine have been identified by a strong peak at 288.5 eV and a small peak at 290.8 eV representing the C—F and CF_2 units, respectively. In the O1s spectrum (see Fig. 8, *b*) two peaks of about equal area found through curve-fitting analysis at 531.8 and 533.4 eV can be associated with the oxygen atom bonded in the C—OH and C=O groups, respectively, and thus confirm the presence of carboxyl groups in F-MWCNT(A)$\cdot$**1**$^{\bullet}$ derivative. The F1s spectrum contains a fairly symmetric peak where curve-fitting analysis yields a major peak at 687.0 eV and a minor peak at 687.6 eV representing residual F atoms bonded in a different environment, such as F—C—C=C and F—C—C structural units on the MWCNT surface.

TGA and DTA studies. These methods use thermal degradation of samples and can provide additional information on the degree of covalent functionalization of materials. Among functionalized carbon nanotubes studied in the present work, SWCNT derivatives seemed to be more suitable for estimation of surface modification by TGA than the multi-walled nanotubes, where only outer surface but not the inner walls are expected to become functionalized by carboxyalkyl groups. Therefore, the following samples of three single-walled carbon nanotubes were selected and studied by TGA: F-XD-SWCNT$\cdot$**1**$^{\bullet}$ (Fig. 9, *a*), F-SWCNT$\cdot$**5**$^{\bullet}$ (Fig. 9, *b*), and F-XD-CNT-**5**$^{\bullet}$ (Fig. 9, *c*).

All TGA curves obtained (Fig. 9) show the major loss in weight due to removal of groups **1**$^{\bullet}$ and **5**$^{\bullet}$ in the temperature range from 150 to 400 °C. The loss in weight is 26% for F-XD-CNT$\cdot$**1**$^{\bullet}$, 13% for F-SWCNT$\cdot$**5**$^{\bullet}$, and 20% for F-XD-CNT$\cdot$**5**$^{\bullet}$, and the corresponding peaks in the DTA curve lie at 232, 255, and 241 °C. The loss in weight at temperatures above 400 °C, most notably exhibited by F-SWCNT-**5**$^{\bullet}$ (Fig. 9, *b*), is associated with removal of the residual fluorine in the form of CF_4 (see Refs 16 and 20). The data on loss in weight give calculated degrees of functionalization (R/C) of 1 : 15 for F-XD-CNT$\cdot$**1**$^{\bullet}$, 1 : 64 for F-SWCNT$\cdot$**5**$^{\bullet}$, and 1 : 32 for F-XD-CNT$\cdot$**5**$^{\bullet}$. The TGA-based R/C value for

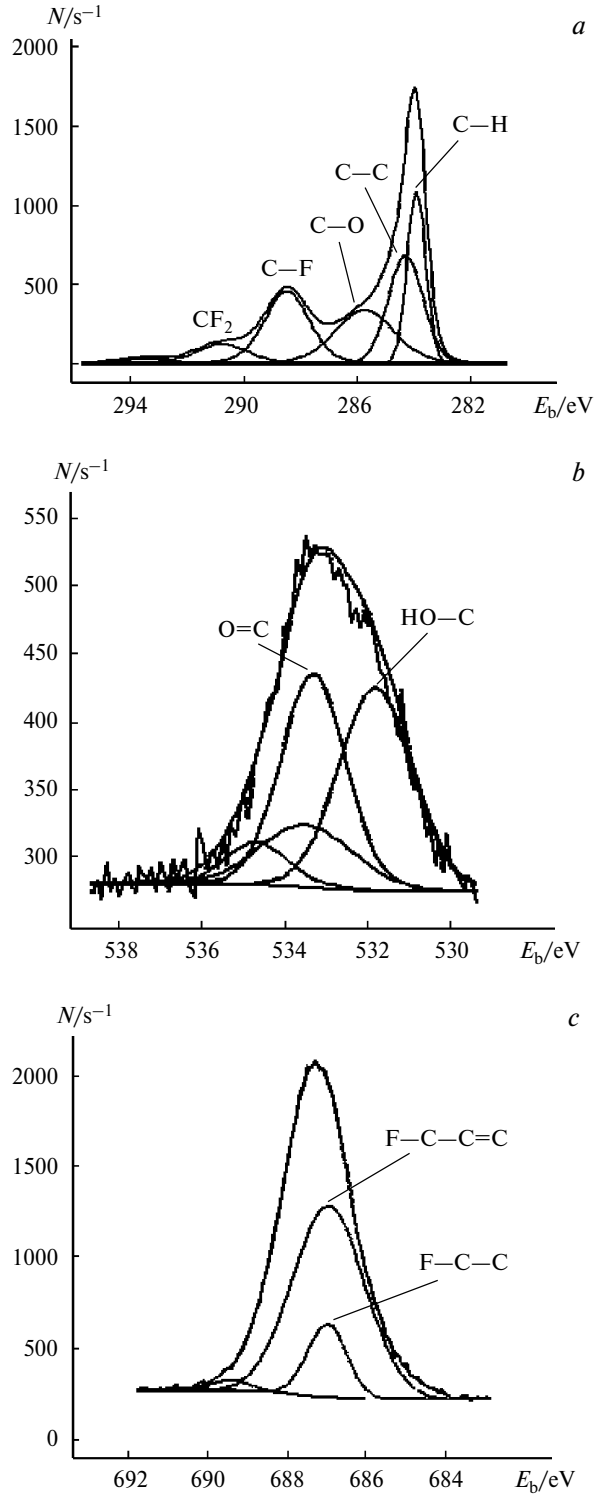

Fig. 8. Curve-fitting analysis of C1s (*a*), O1s (*b*), and F1s (*c*) peaks in the XPS spectra of F-MWCNT($A_{150\,°C}$)·**1**˙. *N* is the number of events per second.

F-SWCNT·**5**˙ is in reasonable agreement with the value calculated from the XPS surface analysis data. Comparison of the R/C value of this derivative with that of

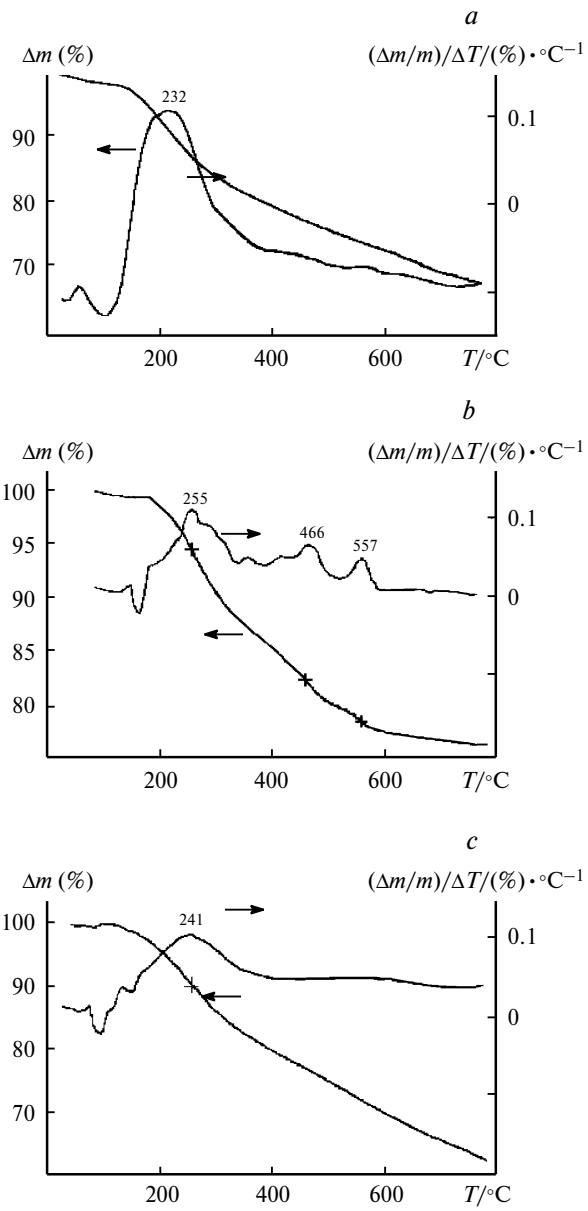

Fig. 9. TGA and DTA plots for alkylcarboxylated CNTs: F-XD-CNC·**1**˙ (*a*), F-SWCNT·**5**˙ (*b*), and F-XD-CNT·**5**˙ (*c*).

F-XD-CNT·**5**˙ leads to conclusion that the lower surface coverage by fluorine in the starting fluoronanotube material (20% in F-XD-CNT) facilitates more efficient cyanopropylcarboxylation of the nanotube surface than in highly fluorinated SWCNTs with C_2F composition. Also, the calculated higher R/C value for F-XD-CNT·**1**˙ than that for F-XD-CNT·**5**˙ is in agreement with the initially assumed higher reactivity of radical **1**˙ relatively to **5**˙ in the reactions with fluoronanotubes.

Solubility. Photographs of the dispersions of functionalized nanotubes in water and polar organic solvents are shown in Fig. 10. The dispersions have been obtained through sonication of 2 mg of each sample in 20 mL of

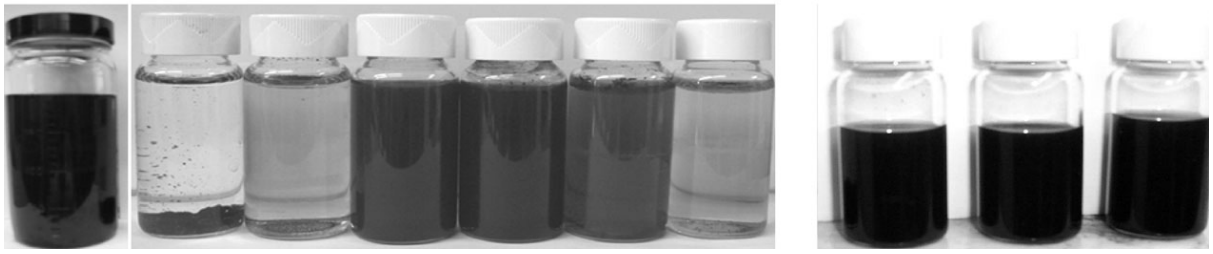

Fig. 10. Photographs of dispersions of functionalized CNTs in water (*a*): F-SWCNT·**5**˙ (*1*), MWCNT (*2*), F-MWCNT(A) (*3*), F-MWCNT($A_{150\,°C}$)·**1**˙ (*4*), F-MWCNT($A_{250\,°C}$)·**1**˙ (*5*), F-MWCNT($B_{150\,°C}$)·**1**˙ (*6*), and F-MWCNT($B_{250\,°C}$)·**1**˙ (*7*) and in polar organic solvents (*b*): F-XD-CNT·**5**˙ (*8*, ethanol; *9*, DMF), and F-XD-CNT·**1**˙ (*10*, DMF).

deionized water, ethanol, or DMF for 1 h. The photographs were taken after storing the suspensions for one week. As shown in Fig. 10, *a*, MWCNTs completely precipitate from water, while F-MWCNTs float on top of water surface. Three out of four different ethylcarboxylated F-MWCNT samples, as well as F-SWCNT-**5**˙ derivative, form stable black-colored suspensions in water in spite of the presence of a substantial amount of residual hydrophobic C—F groups on the nanotube surfaces.

The solubility data obtained are presented in Table 2. They show the highest water solubility (125 mg L^{-1}) not only for F-MWCNT($A_{150\,°C}$)·**1**˙ derivative but also for SWCNT·**5**˙ despite much lower degree of surface functionalization (R/C) by carboxyalkyl groups in the latter. This property can be explained by a much lower density of individually dispersed single-walled nanotubes as compared to multi-walled ones. Therefore, even modest surface coverage by hydrophilic functional groups becomes sufficient for facilitating dispersion and forming stable suspensions in water. The other alkylcarboxylated CNT derivatives, F-XD-CNT·**5**˙ and F-XD-CNT·**1**˙, consisting mostly from single-walled nanotubes showed yet higher solubility in polar organic solvents, ethanol and DMF (up to 1 g L^{-1}), and exhibited intensely black-colored solutions (see Fig. 10, *b*).

Table 2. Solubility of alkylcarboxylated CNTs in water (mg L^{-1})

Compound	Solubility
F-SWCNT·**5**˙	125
F-MWCNT($A_{150\,°C}$)·**1**˙	125
F-MWCNT($A_{250\,°C}$)·**1**˙	25
F-MWCNT($B_{150\,°C}$)·**1**˙	20

***

The obtained data show the advantage of using fluoronanotubes as compared to pristine CNTs for more efficient functionalization through reactions with carboxyalkyl radicals thermally generated from both succinic acid peroxide and 4,4-azobis-(4-cyanovaleric acid). Indeed, this innovative and scalable one-step method is based upon 5—10 times faster chemical reaction rates, thus providing for substantial process energy savings. It was demonstrated that even less reactive free radicals, such as radical **5**˙ produced from compound **6**, can react relatively rapidly (within 24 h) with the fluorinated CNTs, but not at all with the pristine nanotubes. The obtained results show that this method is also very suitable for functionalization of less activated by surface curvature medium and large diameter MWCNTs when they are fluorinated. This finding is particularly attractive if much lower cost of MWCNTs than SWCNTs is taken into account. The developed functionalization method is also non-destructive to the nanotube framework, which is important for applications for CNTs as reinforcing fillers in nanocomposites. Alkylcarboxylated CNT derivatives prepared by this method form stable suspensions in water and polar organic solvents. In addition to nanocomposites, these new CNT derivatives are promising candidates for applications in biomedical research and preparation of water-based paints, inks, and coatings.

This work was financially supported by the NASA Johnson Space Center (Grant NNX07AL50G), Department of Defense SBIR Phase I Program and Award N RUE2-2894-TI-07 from the US Civilian Research and Development Foundation for Independent States of Former Soviet Union (CRDF).

References

1. M. S. Dresselhaus, G. Dresselhaus, P. C. Eklund, *Science of Fullerenes and Carbon Nanotubes*, Academic Press, San Diego, 1996.
2. R. Saito, M. S. Dresselhaus, G. Dresselhaus, *Physical Properties of Carbon Nanotubes*, Imperial College Press, London, 1998.
3. E. G. Rakov, *Russ. Chem. Revs*, 2001, **70**, 827.
4. C. N. R. Rao, B. C. Satishkumar, A. Govindaraj, M. Nath, *CHEMPHYSCHEM*, 2001, **2**, 78.

5. R. Baughman, A. Zakhidov, W. A. de Heer, *Science*, 2002, **297**, 787.
6. M. Meyyappan, *Carbon Nanotube Science and Applications*, CRC Press, 2005.
7. J. N. Coleman, U. Khan, Y. K. Gun´ko, *Adv. Mater.*, 2006, **18**, 689.
8. R. J. Chen, S. Bangsaruntip, K. A. Drouvalakis, N. W. S. Kam, M. Shim, Y. Li, W. Kim, P. J. Utz, H. Dai, *Proc. Natl. Acad. Sci. USA*, 2003, **100**, 4984.
9. B. Vigolo, A. Penicaud, C. Coulon, C. Sauder, R. Pailler, C. Journet, P. Bernier, P. Poulin, *Science*, 2000, **290**, 1331.
10. (a) P. Nikolaev, M. J. Bronikowski, R. K. Bradley, F. Rohmund, D. T. Colbert, K. A. Smith, R. E. Smalley, *Chem. Phys. Lett.*, 1999, **313**, 91; (b) M. J. O´Connell, P. J. Boul, L. M. Ericson, C. B. Huffman, Y. Huang, E. H. Haroz, K. D. Ausman, R. E. Smalley, *Chem. Phys. Lett.*, 2001, **342**, 265.
11. A. Star, J. F. Stoddart, D. Steuerman, M. Diehl, A. Boukai, E. W. Wong, X. Yang, S.-W. Chung, H. Choi, J. R. Heath, *Angew. Chem., Int. Ed.*, 2001, **40**, 1721.
12. A. B. Dalton, C. Stephan, J. N. Coleman, B. McCarthy, P. M. Ajayan, S. Lefrant, P. Bernier, W. J. Blau, H. J. Byrne, *J. Phys. Chem. B*, 2000, **104**, 10012.
13. R. J. Chen, Y. Zhang, D. Wang, H. Dai, *J. Am. Chem. Soc.*, 2001, **123**, 3838.
14. A. Carrillo, J. A. Swartz, J. M. Gamba, R. S. Kane, N. Chakrapani, B. Wei, P. M. Ajayan, *Nano Lett.*, 2003, **3**, 1437.
15. J. L. Bahr, J. M. Tour, *J. Mater. Chem.*, 2002, **12**, 1952.
16. V. N. Khabashesku, W. E. Billups, J. L. Margrave, *Acc. Chem. Res.*, 2002, **35**, 1087.
17. V. N. Khabashesku, J. L. Margrave, *Chemistry of Carbon Nanotubes,* in *Encyclopedia of Nanoscience and Nanotechnology*, Ed. H. S. Nalwa, American Scientific Publishers, 2004, Vol. **1**, 849.
18. V. N. Khabashesku, J. L. Margrave, E. V. Barrera, *Diamond Relat. Mater.*, 2005, **14**, 859.
19. V. N. Khabashesku, M. X. Pulikkathara, *Mendeleev Commun.*, 2006, 61.
20. (a) V. N. Khabashesku, *Fluorination of Carbon Nanotube*, in *Chemistry of Carbon Nanotubes*, Ed. V. A. Basiuk, E. A. Basiuk, ASP Publishers, 2007, Vol. **1**, p. 255; (b) A. V. Krestinin, A. P. Kharitonov, Yu. M. Shul´ga, O. M. Zhigalina, E. I. Knerel´man, M. Dubois, M. M. Brzhezinskaya, A. S. Vinogradov, A. B. Preobrazhenskii, G. I. Zvereva, M. B. Kislov, V. M. Martynenko, I. I. Korobov, G. I. Davydova, V. G. Zhigalina, N. A. Kiselev, *Nanotechnologies in Russia*, 2009, **4**, 115.
21. S. Banerjee, M. G. C. Kahn, S. S. Wong, *Chem. Eur J.*, 2003, **9**, 1898.
22. M. A. Hamon, J. Chen, H. Hu, Y. S. Chen, M. E. Itkis, A. M. Rao, P. C. Eklund, R. C. Haddon, *Adv. Mater.*, 1999, **11**, 834.
23. J. E. Riggs, Z. Guo, D. L. Carroll, Y.-P. Sun, *J. Am. Chem. Soc.*, 2000, **122**, 5879.
24. Y.-P. Sun, W. Huang, Y. Lin, K. Fu, A. Kitaigorodsky, L. A. Riddle, Y. J. Yu, D. L. Carroll, *Chem. Mater.*, 2001, **13**, 2864.
25. A. Hirsch, *Angew. Chem., Int. Ed.*, 2002, **41**, 1853.
26. H. Peng, P. Reverdy, V. N. Khabashesku, J. L. Margrave, *Chem. Commun.*, 2003, 362.
27. H. Peng, L. Alemany, J. L. Margrave, V. N. Khabashesku, *J. Am. Chem. Soc.*, 2003, **125**, 15174.
28. P. Emek, J. W. Seo, K. Hernadi, A. Mrzel, P. Pechy, D. D. Mihailovic, L. Forro, *Chem. Mater.*, 2003, **15**, 4751.
29. Y. Ying, R. K. Saini, F. Liang, A. K. Sadana, W. E. Billups, *Org. Lett.*, 2003, **5**, 1471.
30. J. Zhu, H. Peng, F. Rodriguez-Macias, J. L. Margrave, V. N. Khabashesku, A. Imam, K. Lozano, E. V. Barrera, *Adv. Funct. Mater.*, 2004, **14**, 643.
31. V. N. Khabashesku, H. Peng, J. L. Margrave, W. E. Billups, Y. Ying, US Pat. No. 7,125,533 B2 (issued on Oct. 24, 2006).
32. K. N. Kudun, H. F. Bettinger, G. E. Scuseria, *Phys. Rev. B*, 2001, **63**, 45413.
33. M. Burghard, *Surface Sci. Reports*, 2005, **58**, 1.
34. E. F. Antunes, A. O. Lobo, E. J. Corat, V. J. Trava-Airoldi, *Carbon*, 2007, **45**, 913.

Received August 23, 2011;
in revised form October 26, 2011